

2 **DEVELOPMENT OF PARAMAGNETISM ANALYZER**

3  
4  
5 **Abstract:-**

6 One of the quantities of fundamental importance in describing magnetic  
7 phenomena and materials is the magnetic moment. The research work focused on  
8 the development of a paramagnetic materials analyzer using locally sourced  
9 materials to determine magnetic moment of magnetic materials. The developed  
10 analyser involved the design of a sensing unit. The sensing unit is comprised of a  
11 colpitt oscillator, preamplifier and shaping circuit, K – type thermocouple sensor,  
12 thermocouple amplifier, microcontroller, matrix keypad and a LCD. The designed  
13 colpitt oscillator was used to determine the frequency change for each material  
14 considered. The output analogue signal from the oscillator was fed into the  
15 amplifier and shaping circuit. The shaped output signal from the shaping circuit  
16 was fed into the digital pins of the microcontroller which helps to measure the  
17 period of complete oscillations and hence the frequency. The K – type  
18 thermocouple sensor with a standard sensitivity of  $41 \mu\text{V}/^\circ\text{C}$  was used to  
19 determine the temperature of each paramagnetic material. The measured  
20 temperature was amplified and digitized using Max 6678 thermocouple amplifier  
21 with a resolution of  $0.25 /^\circ\text{C}$  and temperature range of  $-200^\circ\text{C}$  to  $700^\circ\text{C}$ . The  
22 matrix keypad was used to manually enter the mass and atomic mass number of  
23 magnetic samples. The developed instrument was calibrated using a known  
24 standard magnetic moment value of iron. The instrument was tested and it was  
25 able to determine the magnetic moment of available magnetic materials with a  
26 standard deviation of  $0.0163 \pm 0.005$ . The value of magnetic moment obtained for  
27 the available known materials fell within the range of values obtained from  
28 literature. The maximum power consumption of the designed instrument is 3.85  
29 watts.

30  
31 *Magnetic moment, Paramagnetic Material, Oscillator, Microcontroller,*  
32 *Temperature*

33 **1. INTRODUCTION**

34 According to gauss's law of magnetism, there are no monopole sources of magnetic field. Since  
35 there is no magnetic charge, magnetic moment turns out to be a quantity of fundamental  
36 importance in describing magnetic phenomena and materials (Chiou and Williams, 2017). All  
37 substances possess magnetic properties and the ultimate source of their magnetism is the  
38 magnetic moment associated with their atom due to orbital motion and intrinsic spin. The  
39 magnitude of this magnetic moment is dependent on the species of atom. There are many  
40 ingenious and varied ways of realizing the measurement of magnetic moments (Foner, 1967,

41 Bates, 1970). Most common methods for magnetic moment measurement are force method,  
42 induction method and indirect method. Foner (1956) was the first to describe an instrument for  
43 the measurement of magnetic moments; his design has become generic to all subsequent designs  
44 Hoon (1985). Hoon (1985) designed an instrument that can measure magnetic moment of  
45 magnetic materials. It had a robust nature and stability and one which offers great experimental  
46 flexibility. The instrument was calibrated against a known magnetic moment of an annealed high  
47 purity nickel. Pattnaik, (2014) also designed vibrating sample magnetometer, that can measure  
48 magnetic moment at room temperature. The design employed the principle of harmonic vibration  
49 of a magnetic sample in a magnetic field. The harmonicity was achieved by employing a colpitt  
50 oscillator containing sensing coils. The instrument was able to measure magnetic moments of  
51 both ferromagnetic and paramagnetic materials precisely and accurately; it was calibrated against  
52 Nickel. This paper is concerned with developing a paramagnetism analyzer using locally sourced  
53 material to determine magnetic moments of magnetic materials.

54

## 55 **2. MATERIALS AND METHODS**

56 Fig. 1 shows the block diagram of the developed instrument for measurement of magnetic  
57 moment. It comprises of the following (a) a Colpitt's oscillator that generates sinusoidal signal  
58 whose frequency increases or decreases when a magnetic sample poured inside a test tube is  
59 gradually inserted or withdrawn from the oscillator's coil; (b) a buffer amplifier, preamplifier  
60 and shaping circuit which amplifies the signal and shapes it into a square wave using CMOS  
61 Schmitt trigger NAND gate for accurate measurement of wave generated; (c) a thermocouple  
62 sensor which measures the temperature of the material sample and then links it to a  
63 thermocouple amplifier for amplification; (d) a microcontroller which forms the central  
64 processing unit for the whole system. It measures the period of complete oscillations; hence the  
65 frequency of magnetic samples measuring frequency, the temperature and also helps to convert  
66 all analogue signals to digital signal with the aid of analogue – to digital converter and sends  
67 output result to the display; and (e) a liquid crystal display which enables the user monitor the  
68 activity within the microcontroller and as well display the computed value of the magnetic  
69 moment. An automatic battery charger was incorporated to charge the 12 V battery and also act  
70 as a power source supplying 9 V to the entire system. The keypad was used to key in the mass  
71 and atomic mass number of each material sample considered during measurement. The activities  
72 within the microcontroller were controlled using an embedded C – program on arduino platform.

73

74

75

76

77

78

79

80

81

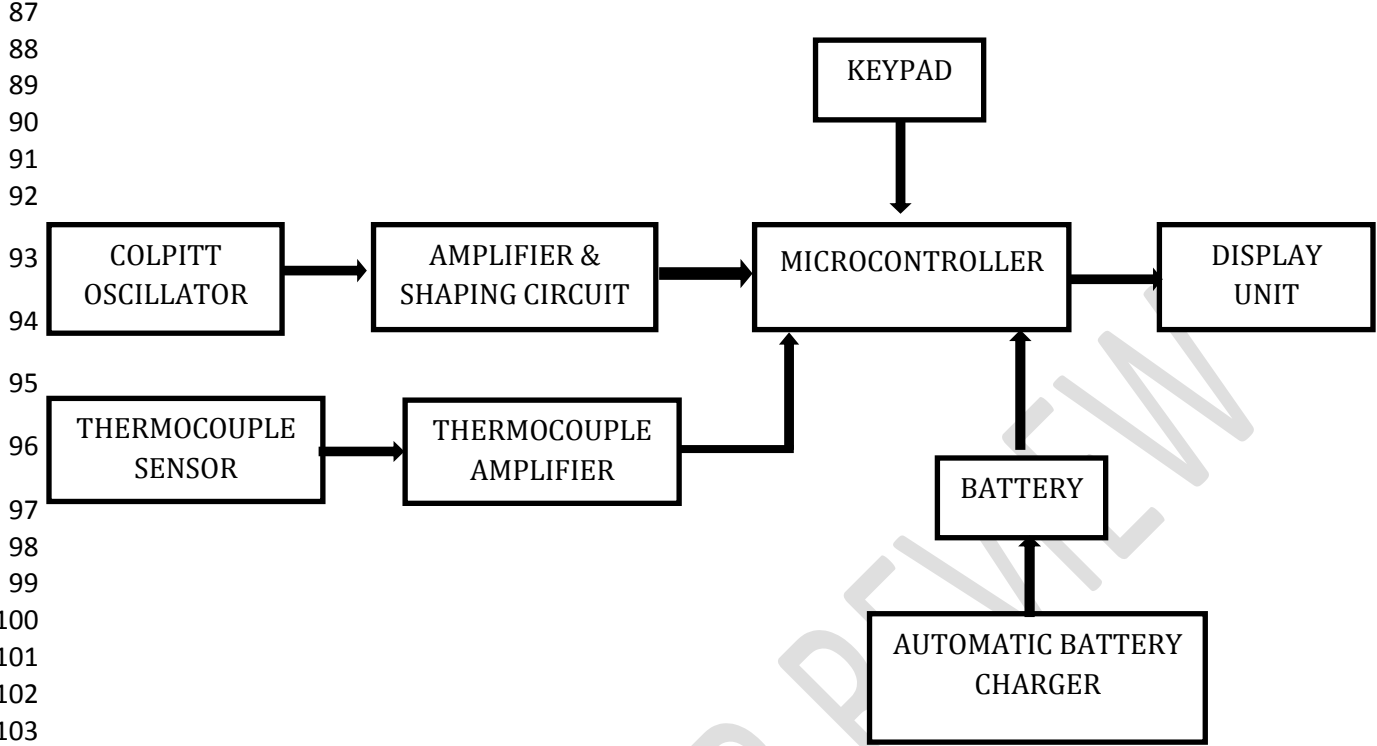
82

83

84

85

86



106 **Figure 1 Complete Block Diagram of the Paramagnetism Analyser**

107  
108  
109  
110  
111 **a) The Oscillator Circuit**

112 The emitter terminal of the transistor is effectively connected to the junction of the two  
113 capacitors, C1 and C2 which are connected in series and act as a simple voltage divider. When  
114 the power supply is firstly applied, capacitors C1 and C2 charge up and then discharge through  
115 the coil L. The oscillations across the capacitors are applied to the base-emitter junction and  
116 appear in the amplified at the collector output. Resistors, R1 and R2 provide the usual stabilizing  
117 DC bias for the transistor in the normal manner while the additional capacitors act as a DC-  
118 blocking bypass capacitors. A radio-frequency choke (RFC) is used in the collector circuit to  
119 provide a high reactance (ideally open circuit) at the frequency of oscillation, (  $f_r$  ) and a low  
120 resistance at DC to help start the oscillations. The required external phase shift is obtained from  
121 positive feedback obtained for sustained undamped oscillations. The amount of feedback is  
122 determined by the ratio of C1 and C2. These two capacitances are generally “ganged” together to  
123 provide a constant amount of feedback so that as one is adjusted the other automatically follows.  
124

125  
 126  
 127  
 128  
 129  
 130  
 131  
 132  
 133  
 134  
 135  
 136  
 137

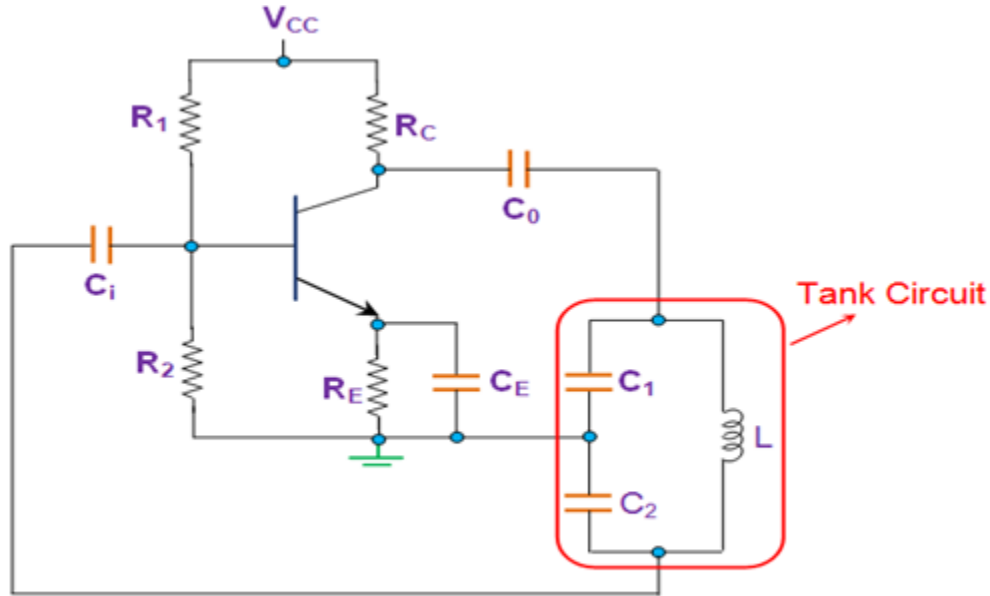


Figure 2 Colpitts Oscillator

138

139 In the design of the colpitts oscillator circuit, a single stage full biasing bipolar transistor  
 140 amplifier (NPN) was used to produce a sinusoidal output. The capacitive voltage divider in  
 141 the tank circuit works as the feedback source. The design Considerations for figure 2 are as  
 142 follows:

143  $V_B = 3.2 \text{ V}$ ,  $I_B = 0.87 \text{ mA}$ ,  
 144 Assuming  $I_C \approx I_E$

$$V_E = 10\%V_{CC} \quad 1$$

145 The biasing resistors were obtained using the following expressions:

$$R_1 = \frac{V_{CC} - V_B}{I_B} \quad 2$$

$$R_2 = \frac{V_B R_1}{V_{CC} - V_B} \quad 3$$

$$R_E = \frac{V_B - V_{BE}}{I_E} \quad 4$$

$$R_B = R_1 // R_2 \quad 5$$

$$\text{Stability factor} = \frac{R_B + R_E}{R_E} = 10 \quad 6$$

146 The values of  $R_1$ ,  $R_2$ , and  $R_E$ , are 10k, 3.7k, and 580 respectively.

147 The frequency of oscillations was obtained using:

$$f_r = \frac{1}{2\pi\sqrt{LC_T}} \quad 7$$

148 The frequency of interest is 2 MHz; the capacitors  $C_1$  and  $C_2$  were selected such that the gain is  
149 10 knowing that:

$$Gain = \frac{C_2}{C_1} \quad 8$$

150 The inductance of the inductor L was obtained using equation 1.9.

$$L = \frac{1}{4\pi^2 f_r^2 C_T} \quad 9$$

151 Where

$$C_T = \frac{C_1 C_2}{C_1 + C_2} \quad 10$$

152 The value of the inductance of the inductor L obtained is 0.0696 nH and capacitors  $C_1$  and  $C_2$   
153 are 27 nF and 270 nF respectively.

154 The number of turns for the air core coil with inductance value gotten above was calculated  
155 using the expression below:

$$L = \frac{0.394r^2 N^2}{9r+10l} \quad 11$$

157 where r is the radius of the air core coil, l is the length of the air core coil and N is the number of  
158 turns. The selection of gauge of the copper wire depends on the current that passes the inductor.  
159 A single wire gauge of 40 was used with a maximum current capacity of 23.3 mA.

160

### 161 b) Amplifier & Shaping Circuit

162 This circuit consists of an emitter follower, amplification and shaping circuit is figure 3. To  
163 improve the weak output signal from the oscillator, the emitter follower was placed between the  
164 oscillator and the amplification circuit since it is usually characterized by high input impedance  
165 and low output impedance. The following parameters were considered for the emitter follower  
166 and amplifier with shaping circuit design.

167  $V_B = 2.1 V$ ,  $I_B = 10 \mu A$ ,  $hfe = 100$ ,  $V_{CC} = 5 V$ ,  $V_{BE} = 0.7 V$

$$R_5 = \frac{V_{CC} - V_B}{I_B} \quad 12$$

$$R_6 = \frac{V_B - V_{BE}}{I_E} \quad 13$$

168 Where  $I_E = I_B hfe$

169 Required resistors values are  $R_5 = 290 k\Omega$  and  $R_6 = 1.4 k\Omega$

170 The amplification section is a simple common emitter amplifier because of its best combination  
 171 of voltage gain and current gain.

172  $I_B = 4.3 \mu A, hfe = 270, V_C = \frac{1}{2} V_{CC} = 4.5 V$

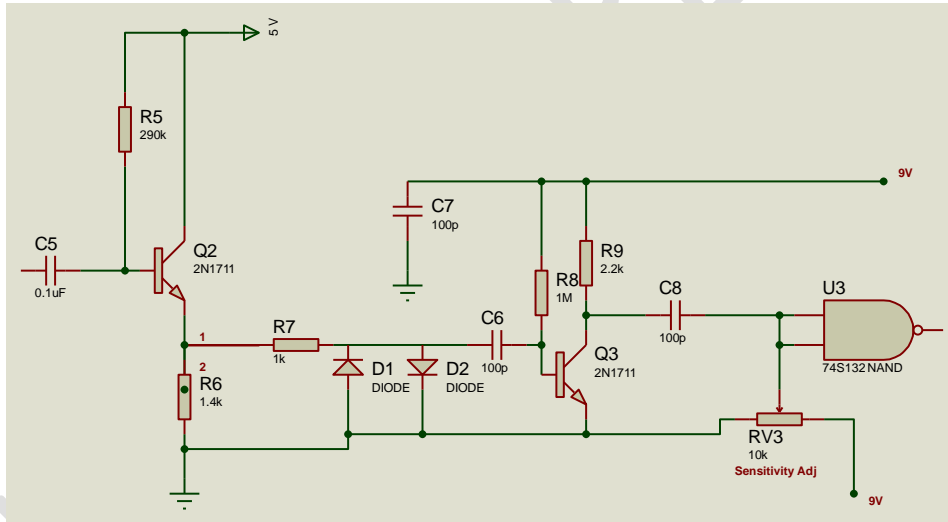
$$R_6 = \frac{V_{CC} - 0.7 V}{I_B} \tag{14}$$

$$R_7 = \frac{V_{CC} - V_C}{I_C} \tag{15}$$

173 Where  $I_C = I_B hfe$

174 The required value of  $R_7$  and  $R_8$  are 1 MΩ and 2.2 kΩ respectively.

175 The shaping circuit unit was implemented using 74S132 CMOS Schmitt trigger NAND gate.  
 176 When the voltage from the output of the emitter follower reaches 1.8 V, the NAND gate is high  
 177 until it's below noise margin level thereby producing square wave. This square waveform is fed  
 178 into microcontroller. To obtain the frequency of oscillation, the microcontroller determines the  
 179 period when the signal is HIGH and LOW.



180  
181  
182  
183  
184  
185  
186  
187  
188  
189  
190 Fig. 3 Amplifier & Shaping Circuit

191 **c) Temperature Sensing**

192 Several types of temperature sensing techniques exist. This research work utilizes the thermo-  
 193 junction Type K (chromel–alumel) temperature sensor. This sensor offers a wide temperature  
 194 range, has low standard error, and has good corrosion resistance. The circuit in Figure 4 is a  
 195 single-supply, type k thermocouple signal conditioning circuit with cold-junction compensation.  
 196 It conditions the output of a Type K thermocouple, while providing cold-junction compensation  
 197 for temperatures between 0°C and 250°C. The circuit operates from a single 3.3 V to 5.5 V  
 198 supply and is designed to produce an output voltage transfer characteristic of 10 mV/°C. A Type  
 199 K thermocouple exhibits a Seebeck coefficient of approximately 41 μV/°C; therefore, at the cold  
 200 junction, the TMP35 (low voltage, precision centigrade temperature sensor), with a temperature  
 201 coefficient of 10 mV/°C, is used with  $R_1$  and  $R_2$  to introduce an opposing cold-junction

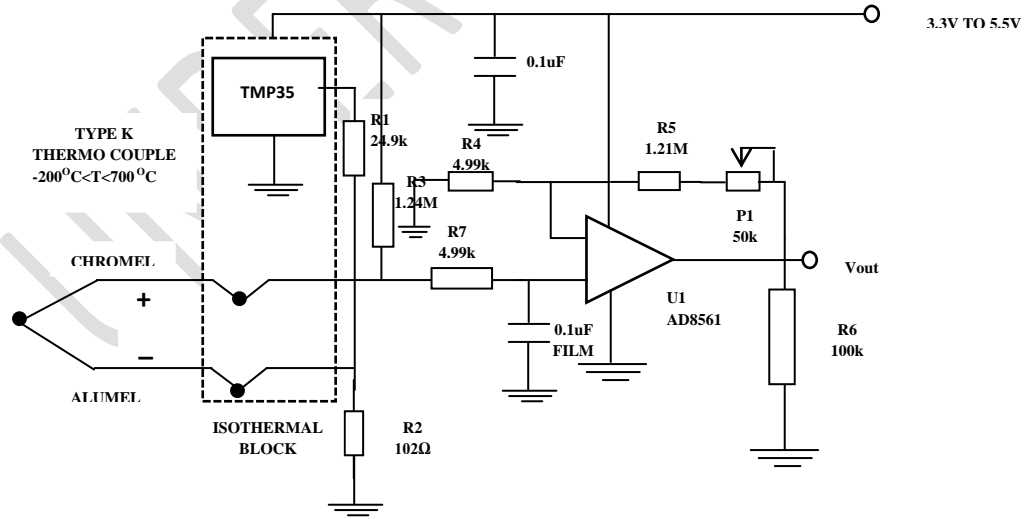
202 temperature coefficient of  $-41 \mu\text{V}/^\circ\text{C}$ . This prevents the isothermal, cold-junction connection  
 203 between the PCB tracks of the circuit and the wires of the thermocouple from introducing an  
 204 error in the measured temperature. This compensation works extremely well for circuit ambient  
 205 temperatures in the range of  $20^\circ\text{C}$  to  $50^\circ\text{C}$ . Over a  $250^\circ\text{C}$  measurement temperature range, the  
 206 thermocouple produces an output voltage change of  $10.151 \text{ mV}$ . Because the required output  
 207 full-scale voltage of the circuit is  $2.5 \text{ V}$ , the gain of the circuit is set to  $246.3$ . Choosing  $R_4$  equal  
 208 to  $4.99 \text{ k}\Omega$  sets  $R_5$  equal to  $1.22 \text{ M}\Omega$ . Because the closest 1% value for  $R_5$  is  $1.21 \text{ M}\Omega$ , a  $50 \text{ k}\Omega$   
 209 potentiometer is used with  $R_5$  for fine trim of the full-scale output voltage. Although the OP193  
 210 is a superior single-supply, micropower operational amplifier, its output stage is not rail-to-rail;  
 211 therefore, the  $0^\circ\text{C}$  output voltage level is  $0.1 \text{ V}$ . The circuit is digitized by a single-supply ADC,  
 212 by adjusting the ADC common to  $0.1 \text{ V}$ .

213 **d) Display unit**

214 A  $16 \times 2$  LCD unit compatible with the Hitachi HD44780 driver was adapted for use as the  
 215 display unit for the developed instrument. The LCD output was controlled by an arduino  
 216 microcontroller unit which has an inbuilt ADC unit for converting analogue signals to digital  
 217 signals. The Arduino microcontroller used a liquid crystal library to control the LCD display.  
 218 The microcontroller manipulates several interface pins at once to control the display.

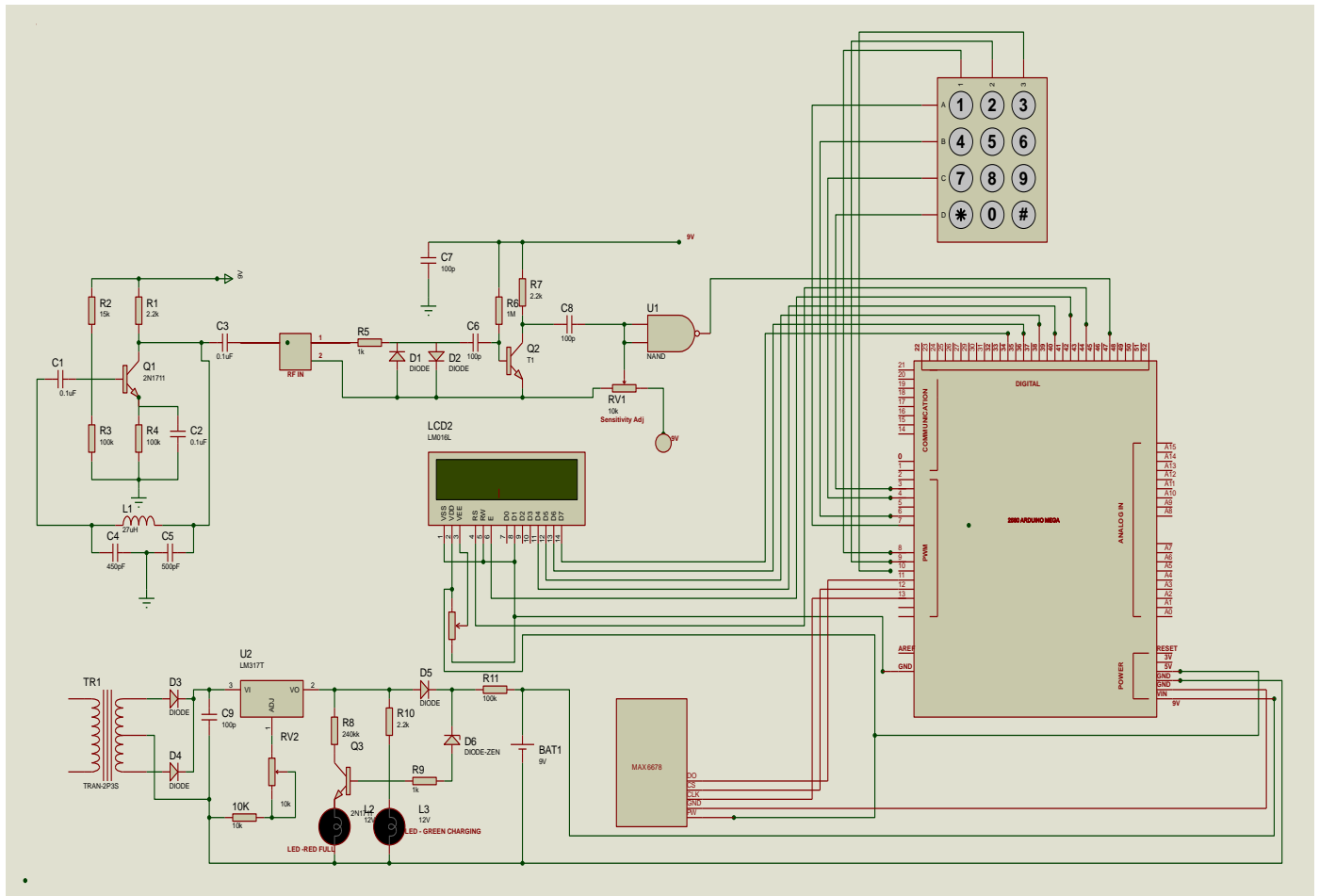
219 **e) Microcontroller**

220 For this research work, a 2560 arduino mega microcontroller was used owing to its flexibility,  
 221 availability and huge libraries database. It functions as a frequency counter and thermometer by  
 222 measuring the frequency of oscillation whenever magnetic materials are introduced into the  
 223 oscillator's coil and temperature required to compute magnetic moment of magnetic samples. A  
 224 suitable micro-C code was written and embedded in the microcontroller so as coordinate the  
 225 activity of the entire system, perform the necessary calculations and send output result to the  
 226 display unit. The microcontroller was interfaced with a 2 by 16 Hitachi Liquid Crystal Display  
 227 (LCD) so as to display the measured values of magnetic moment.



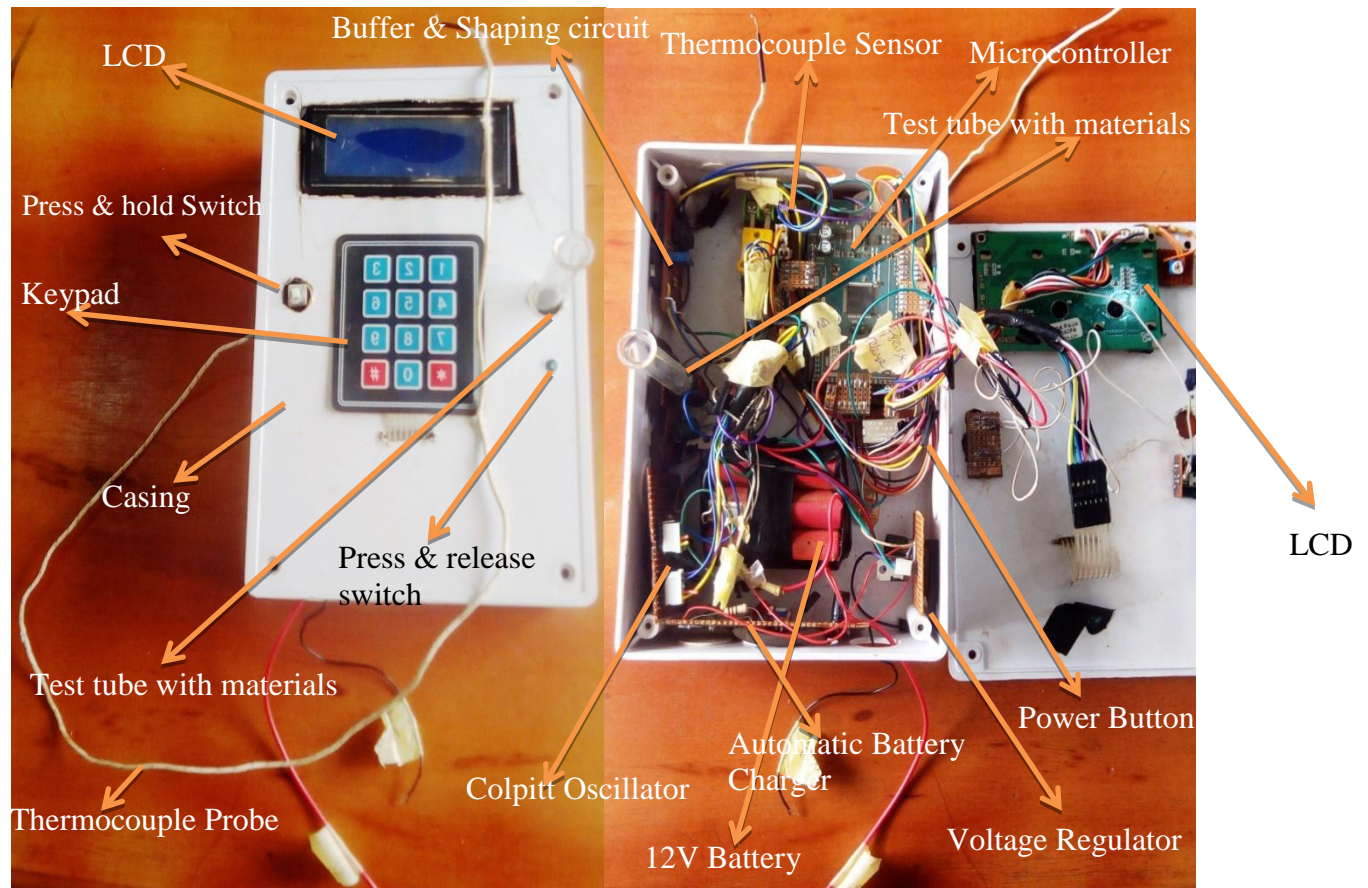
245 Figure 4: Thermocouple Amplifier

246



247  
248

Figure 5: Complete Circuit Diagram of the Developed Paramagnetism Analyser.



249

250 Figure 6: Image of the developed Paramagnetism Analyzer

251 **3. TESTING, PERFORMANCE EVALUATION AND CALIBRATION**

252 **a) Testing and Examination of Counter Developed and Oscillator Circuit**

253 The figure 5 shows the completed circuit of the developed paramagnetism analyser under test  
 254 and evaluation. Table 1 shows the data obtained from the analysis carried out during the testing  
 255 of the digital counter developed and available digital frequency meter. The testing was done by  
 256 simultaneously passing a varying signal from a standard signal generator into the developed  
 257 frequency counter and a standard frequency meter (MEGGER M7029) to verify if there is  
 258 variation between the two measurements. Although the actual measurement recorded by the two  
 259 instruments differs a little due to marginal discrepancy, however there is a consistency in the  
 260 variation of two sets of measurement with respect to the input signal from the signal generator.  
 261 The factor by which the measurement of the standard frequency meter increases or decreases is  
 262 the same factor by which the measurement of the designed meter increases or decreases. The  
 263 correlation factor ( $R^2$ ) obtained from table 1 is 0.99950, show a reliably good agreement between  
 264 the measured values with the standard data values. Statistical analysis revealed a mean  
 265 percentage error value of 1.17% and accuracy of 98.83%. This shows that the designed  
 266 frequency counter compared favorably well with the standard frequency meter (MEGGER  
 267 M7029). The comparison plot of standard frequency meter against the designed frequency  
 268 counter was plotted on an excel spreadsheet and the graph is shown in Figure. 7.

269

270 **Table 1: The output frequency from the developed frequency counter and the standard**  
 271 **meter with respect to the varying input signal from the signal generator and the errors**

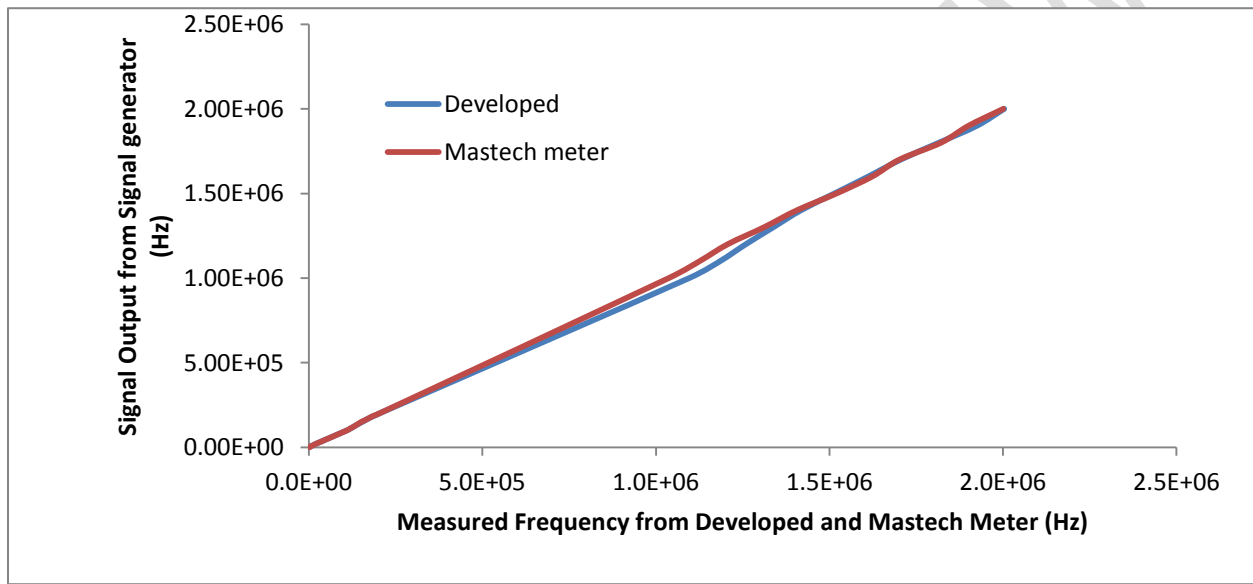
Signal Generator (Hz)	Designed Counter (Hz)	Standard Meter(Hz)	Error
1.0K	1088	1072.7	0.01426307
1.1K	1185	1164.8	0.01734203
1.2K	1259	1241.3	0.01425924
1.3K	1341	1311.2	0.02272727
1.4K	1414	1407.8	0.00440403
1.5K	1520	1520.8	0.00052604
1.6K	1612	1605.4	0.00411112
1.7K	1723	1705.8	0.01008325
1.8K	1812	1805.9	0.00337782
1.9K	1922	1901.9	0.01056838
2.0K	2011	2002.6	0.00419455
10K	10805	10605.0	0.01885903
11K	11765	11524.0	0.02091288
12K	12393	12410.0	0.00136986
13K	13254	13216.0	0.0028753
14K	14059	14285.0	0.01582079
15K	15050	15272.0	0.01453641
16K	16143	16529.0	0.02335289
17K	17029	17349.0	0.01844487
18K	18062	18008.0	0.00299867
19K	19040	19086.0	0.00241014
20K	20230	20176.0	0.00267645
100K	110004	110330.0	0.00295477
110K	119482	118600.0	0.00743676
120K	127780	127910.0	0.00101634
130K	136467	135720.0	0.00550398
150K	154168	151420.0	0.01516921
160K	163226	161920.0	0.0181482
170K	171929	171500.0	0.00806571
180K	181696	180380.0	0.00250146
190K	192921	191770.0	0.00729571
200K	203359	203350.0	0.00600198
1.0M	1096355	1037500.0	4.4259E-05
1.1M	1185157	1126300.0	0.05672771
1.2M	1259316	1207300.0	0.05225695
1.3M	1338146	1311500.0	0.04308457
1.4M	1417516	1405900.0	0.02031719
1.5M	1514649	1520800.0	0.00826232
1.6M	1612017	1623500.0	0.00404458
1.7M	1705464	1701800.0	0.00707299

1.8M	1815580	1821900.0	0.00215301
1.9M	1924996	1901100.0	0.00346891
2.0M	2003709	2001200.0	0.01256956
		0.99950	0.01172

272

273 Figure. 7: Comparative plot of developed Frequency Counter against Standard Frequency meter  
 274 with respect to a varying signal generator.

275 The oscillator's response was examined when a magnetic material is introduced into its coil by



276 gradually lowering granulated magnetic material contained in a test tube inside the oscillators  
 277 coil. This causes a change in the inductance of the coil which in turn causes changes in the  
 278 output frequency of the oscillator. The corresponding frequency values were measured using  
 279 both the standard frequency meter (MEGGER M7029) and the developed oscillator with counter.  
 280 The results obtained are shown in Table 2. Obviously from the table 2, the result showed that the  
 281 developed oscillator with counter compared favorably well with one obtained with the standard  
 282 frequency meter. That means that oscillator is fairly stable and reliable.

283

284

285

286

287

288

289

290

291 **Table 2 Frequency Count from both Meters when Sample Materials were gradually**  
292 **lowered into the Coil**

Frequency Counter	Frequency Meter	Deviations
1502813	1502712	6.72118E-05
1512812	1512701	7.33787E-05
1601812	1601702	6.86769E-05
1661281	1661171	6.62183E-05
1700302	1700221	4.76409E-05
1700412	1700302	6.46944E-05
1801328	1801218	6.10698E-05
1802787	1802621	9.20881E-05
		0.0000676

293

294 **b) Calibration of Paramagnetic Analyser**

295 The developed instrument was calibrated using iron as a standard magnetic sample with known  
296 magnetic moment value as provided in literature. It is necessary to compute the calibration  
297 constant K in order to ascertain the accuracy and efficiency of the developed system. The  
298 calibration of the paramagnetic analyzer was done using equation 16

$$\mu_{eff} = \frac{KT M_r \Delta f}{m f_0} \quad 16$$

299 Where  $\mu_{eff}$  is the effective magnetic moment ( $Am^2$ ), K is the calibration constant ( $Am^2/K$ ),  
300  $M_r$  is the atomic mass (kg), T is the Temperature (K),  $\Delta f$  is the frequency change (Hz), m is  
301 the mass of sample materials (kg). The microcontroller was used to measure the frequency and  
302 temperature; the mass of sample material was obtained using an electronic balance. These made  
303 the computation of the calibration constant easier. The following procedures were observed:  
304 firstly, the mass and the temperature of the material samples were determined using an electronic  
305 balance and a temperature sensor respectively. Thereafter, the frequency of the oscillator when  
306 an empty tube was inserted and when a known mass of known material with known magnetic  
307 moment was inserted were measured and this gave the frequency change. The table 3 gives the

308 record of the measured and constant parameters. The calibration constant was computed using  
 309 the expression below and was incorporated into the microcontroller for accurate computations of  
 310 magnetic moment for the available materials considered.

311 **Table 3: Parameters for Calibration Constant Computation**

Parameter	Values
Initial frequency, $f_0$ (Hz)	1502813
Final frequency, $f_f$ (Hz)	1802787
Frequency change, $\Delta f$ (Hz)	299974
Measured mass, $m$ (kg)	0.005
Obtained atomic mass number, $M_r$ (kg)	0.056
Obtained magnetic moment of known sample $\mu_{eff}$ , ( $Am^2$ )	5.60
Temperature, $T$ (K)	303

$$\text{Calibration constant, } K = \frac{\mu_{eff} m f_0}{M_r T \Delta f} = 0.00000185 \text{ } Am^2/K \quad 17$$

312 This value was incorporated into the microcontroller for accurate computation of the magnetic  
 313 moment of the available material considered.

#### 314 4. RESULT

315 **Table 4: Measured and standard magnetic moment of magnetic materials available**

Materials	Measured $\mu_{eff}$ ( $Am^2$ )	<sup>[1]</sup> Standard $\mu_{eff}$ ( $Am^2$ )
Aluminium	3.65	3.63 – 4.00
Copper	1.99	1.90 – 2.10
Iron	5.70	5.00 – 5.60

316 [1] <http://web.uvic.ca/~djberg/Chem324/Chem324-12.pdf>

#### 317 5. MEAN STANDARD DEVIATION ESTIMATION

318 The mean standard deviation of the designed instrument was obtained by repeatedly measuring  
 319 the magnetic moment of a magnetic sample (iron) for good ten times in order to test repeatability  
 320 or deviation from true value. The repeated measured values obtained are shown in table 5

321

322 **Table 5: Mean Standard deviation Table.**

Measured values ( $x$ )	$x_i - \bar{x}$	$(x_i - \bar{x})^2$
5.70	0.015	$2.25 \times 10^{-4}$
5.69	0.005	$2.50 \times 10^{-5}$
5.70	0.015	$2.25 \times 10^{-4}$
5.65	- 0.035	$1.23 \times 10^{-3}$
5.68	- 0.005	$2.50 \times 10^{-5}$
5.71	0.025	$6.25 \times 10^{-4}$
5.67	- 0.015	$2.25 \times 10^{-4}$
5.68	- 0.005	$2.50 \times 10^{-5}$
5.69	0.005	$2.50 \times 10^{-5}$
5.68	- 0.005	$2.50 \times 10^{-5}$
		$2.655 \times 10^{-3}$

323

324 Standard deviation ,  $\sigma = \sqrt{\frac{1}{N} \sum_{i=1}^N ((x_i - \bar{x})^2)} = \sqrt{\frac{2.655 \times 10^{-3}}{10}} = 0.0163 \approx 0.02$

$$\text{Standard deviation error, } \mu = \frac{\sigma}{\sqrt{n}} = \frac{0.0163}{\sqrt{10}} = 0.005$$

325 **6. DISCUSSION**

326 The colpilt oscillator was designed to give an output frequency of 2 MHz and above with a  
 327 resolution of 1 Hz. Obviously from Table 1, the designed oscillator with counter compared  
 328 favorably well with the standard frequency meter (MEGGER M7029). Although the actual  
 329 readings recorded by the two instruments differ a little due to marginal discrepancy, however  
 330 there is a consistency in the variation of the two sets of measurement with respect to the input  
 331 signal from the signal generator. The factor by which the measurement of the standard frequency  
 332 meter increases or decreases was the same factor by which the measurement of the designed  
 333 meter increases or decreases as shown in Figure 1. Statistical analysis revealed a mean  
 334 percentage error value of 1.17% and accuracy of 98.83%. The correlation factor ( $R^2$ ) of 0.99950  
 335 obtained also show a reliably good agreement between the designed oscillator with counter  
 336 measured values and the standard meter measured values. The oscillator's performance and

337 response when a magnetic material is introduced into its coil were also verified. This was  
338 achieved by gradually lowering granulated magnetic material contained in a test tube inside the  
339 coil of the oscillators. This causes a change in the inductance of the coil which in turn causes  
340 changes in the output frequency of the oscillator. The corresponding frequency values were  
341 measured using both the standard frequency meter (MEGGER M7029) and the developed  
342 oscillator with counter. The results obtained are shown in Table 2. Obviously from the table, the  
343 result showed that the developed oscillator with counter compared favorably well with the  
344 standard frequency meter with an absolute mean deviation of 0.0000676. This means that when  
345 any material that has paramagnetic or ferromagnetic properties inserted into the coil of the  
346 oscillator there will be a corresponding frequency change. The temperature sensing device used  
347 measures temperature between  $-200^{\circ}\text{C}$  to  $700^{\circ}\text{C}$  with a sensitivity of  $41\ \mu\text{V}/^{\circ}\text{C}$  and a resolution  
348 of  $0.25/^{\circ}\text{C}$ . To ascertain the accuracy and efficiency of the developed system, the instrument  
349 was calibrated using iron as a standard magnetic sample with known magnetic moment value.  
350 The calibration constant K was computed and the value obtained is  $0.00000185\text{A}/\text{m}^2$ . After the  
351 design, examination and performance test was carried out on the developed paramagnetism  
352 analyzer. It was found that the instrument measures the magnetic moment of the materials  
353 available accurately with a resolution of  $0.01\ \text{A}/\text{m}^2$  and a mean standard deviation of  
354  $0.0163\pm 0.005$ . This means that error in the instrument is very insignificant and that it can  
355 accurately measure magnetic of magnetic materials once without repeated measurements. The  
356 standard deviation was obtained using Table 5 by repeatedly measuring the magnetic moment of  
357 the magnetic samples tested for ten numbers of times. The results are shown in Table 4.  
358 Obviously from the table, the measured values of magnetic moment for the available known  
359 materials fall within the range of values obtained from literature. In the case of iron, a difference  
360 of  $0.1\text{Am}^2$  was observed. This may be as a result of impurities arising from metal recycling  
361 processes. The maximum power consumption of the developed instrument is 3.85 watts.

## 362 CONCLUSION

363 The aim of this study was carried out to a conclusive end. This involves the design and  
364 construction of a paramagnetism analyzer. The developed instrument showed a good response  
365 and the performance was excellent when the measured magnetic moment values were compared  
366 with existing standard magnetic moment values obtained from literature with a standard  
367 deviation of  $0.0163\pm 0.005$  and a resolution of  $0.01\text{Am}^2$ . Aluminum had a magnetic moment of  
368  $3.65\ \text{Am}^2$ , copper had  $1.99\ \text{Am}^2$  and Iron had  $5.70\ \text{Am}^2$ . The correlation factor ( $R^2$ ) of 0.99950  
369 obtained for the two frequency counter also show a reliably good agreement between the  
370 designed frequency counter measured values and the standard meter measured values. Statistical  
371 analysis revealed a mean percentage error value of 1.17% and accuracy of 98.83%. The  
372 temperature sensing device measures temperature between  $-200^{\circ}\text{C}$  to  $700^{\circ}\text{C}$  with a sensitivity of  
373  $41\ \mu\text{V}/^{\circ}\text{C}$  and a resolution of  $0.25/^{\circ}\text{C}$ . Conclusively therefore, the instrument performed well  
374 and it is recommended for measurement of magnetic moment of magnetic sample (ferromagnetic  
375 and paramagnetic) in material science/condensed matter laboratories. The developed instrument  
376 is a portable handheld device which operates well on a rechargeable DC power source. It is  
377 cheap, easy to repair if malfunctioned and does not require any special skill to operate.

378

379

380 **REFERENCES**

- 381 Chiou Lawrence and Christopher Williams (2017); Magnetic moment. Brilliant.org. Retrieved  
382 15:49, August 15, 2017 from [https://brilliant.org/wiki/magnetic - moment/](https://brilliant.org/wiki/magnetic-moment/).
- 383 Foner, S. (1959); Versatile and Sensitive vibrating Sample Magnetometer. *Rev. Sci. Instrum.*  
384 30(7), 546 – 557.
- 385 Hoon, S. R. (1983); An inexpensive, sensitive vibrating sample magnetometer. *The Institute of*  
386 *Physics and the European Physical Society*. Vol. 4, page 61 – 62
- 387 Magnetism in Transition Metals complexes; retrieve from [https://web.unic.ca/ djberg/Chem324-](https://web.unic.ca/~djberg/Chem324-12.pdf)  
388 12.pdf retrieve on 12th February, 2017, 3:22 pm.
- 389 Pattnaik . D. P. (2014); *Design and Fabrication of Vibrating Sample Magnetometer*. Department  
390 of Physics and Astronomy, National Institute of Technology, Rourkela 769008, Odisha,  
391 India.

393

394

395

396

397

398